



Type of the Paper (Article)

Green nano-coated carbon electrodes for detecting furosemide drug

Dhafer Jassim Mohammed¹, Ali Ibraheem Khaleel², Shatha Y. Al-Samarrai^{2*}

¹Directorate of Babylon Education, Ministry of Education, Babylon, Iraq.

²Chemistry Department, College of Science, Tikrit University, Iraq.

*Corresponding Author: dr.shatha81@tu.edu.iq

Received date: 18/03/2024; Accepted date: 30/03/2024; Published date: 31/03/2024

Abstract: In this study, new coated carbon electrodes were created and utilized to estimate the furosemide (FUR) drug. Ion-pair preparation for the electrode construction involved a reaction of furosemide drug with silver nanoparticles (Ag-NPs) made from pomegranate peel extract, plasticizers that use dibutyl phthalate (DBP) without the use of any organic precipitant. Several techniques (AFM, XRD, FTIR, SEM) were used to characterize the characteristics. This electrode shows excellent sensitivity to furosemide (FUR) with a linear range of 10^{-6} - 10^{-1} M and a correlation coefficient of 0.9798. The electrode has a lifetime of 45 days, ideal temperatures of 20-45 °C, an optimum pH range of 3-6, a slope of 61.286 mv/decade, and a detection limit of 3.62×10^{-8} M. The AFM was measured, the total height was 2.53 nm, and the shape was spherical or semi-spherical. The average crystal size measured by XRD was 43.52, 47, and 55.03 nm with an average size of 14.25067 nm; the particles were spherical or semi-spherical in shape, as seen using the SEM. The identification of functional aggregates was conducted by measuring them using FTIR. In conclusion, this method could be an efficient tool for determining the drug in pharmaceutical formulations.

Keywords: Green synthesis; Pomegranate peel; silver nanoparticles.

1. Introduction

Furosemide (FUR) is commonly used to treat edema brought on by heart failure and hepatic or renal issues. It is a strong loop diuretic (1), and patients who are not responding to thiazide diuretics may find it useful (2). The half-life period can be as long as two hours, while individuals with renal and hepatic impairment experience a longer half-life, furosemide is chemically known as 4-Chloro-2-(furan-2-ylmethylamino)- 5-sulfamoyl benzoic acid (3), the molecular weight of 330.77, the empirical formula is $C_{12}H_{11}ClN_2O_5S$, it ranges in color from white to slightly yellow (4).

It works by inhibiting the Na^+ , K^+ , and $2Cl$ cotransporter in the thick ascending limb of the loop of Henle, resulting in increased water excretion together with sodium, chloride, and potassium (5-7).

A variety of techniques have been described for the determination of (FUR) in Pharmaceutical Dosage by samples (HPLC) (8,9), atomic absorption and UV-visible spectrophotometry (10), voltammetry (11,12), and LC-ESI-MS (13).

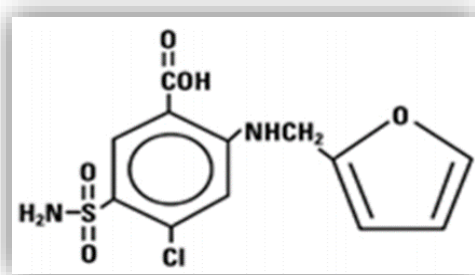


Figure 1: The chemical structure of Furosemide (FUR)

Particles having a structural size of 100 nm or less are referred to as nanoparticles (14), Silver Nanoparticles used in its unique and antibacterial properties, is widely used in several applications Nanosilver is utilized in medical devices, clothes, cosmetics, electronics, biosensing, and other products (15). AgNPs are harmful to a variety of cultured mammalian cells, according to in vitro research, but the toxicity of silver nanoparticles can be decreased by the green synthesis of AgNPs(16). The search aims to build a nanoelectrode and utilize it to calculate the drug (Fur) in the presence of Nanosilver using the selective ion technique without the need for chemical precipitants.

2. Materials and Methods.

2.1. Instrumentations

Potentiometric evaluations were done utilizing a Jenway3545 pH meter, calomel electrodes No HI5412 (Italy), Hot plate with magnetic stirrer LMS-1003(Germany), and Sensitive balance SHINKO-GS (Japan).

2.2. Reagents and solutions

All of the compounds were of the analytical reagent quality; the creation of stock solutions required the use of distilled water. The following resources: FUR (SDI, samara-Iraq) Polyvinyl chloride (PVC), high purity (Fluka), Di-butyl phthalate (Fluka), Tetra hydro furan (THF) (Sigma), Sodium hydroxide (BDH), and Silver nitrate (Sigma). In this work, A stock solution of 0.1 M of FUR drug was prepared by dissolving 3.3077 gm in a dilute solution of alkali hydroxide and then completing to 100 ml distilled water solutions (1.0×10^{-6} - 1.0×10^{-2}) M of the drug by dilution with D.W, LaSiX tablets (40 mg furosemide) pharmaceuticals from India from local pharmacies, were bought.

2.2. Sample Preparation

Ten tablets of LaSiX tablets 40 mg furosemide (weight of all tablets 2.4365gm) finely ground and thoroughly combined with 0.2436g of LaSiX was prepared by dissolving in a dilute solution of alkali hydroxide then completed to 100 ml distilled water. The resultant mixture was then filtered using Whatman filter paper, then water was added to the 100-mL volumetric flask to finish the volume to the mark. Concentration of the resulting solution 10^{-3} M Other concentrations were created by appropriately diluting them with distilled water.

2.3. Preparation of pomegranate peel extract.

The fruits were cut and washed in ultrapure water; the arils were removed from the peels; the peels were divided into little bits, take 20 gm from the peels, and added 400 ml distilled water,



boiled for 15 minutes at 70–75 °C, then let to cool followed by Whatman NO1 filtering, a light-yellow extract was produced.

2.4. Preparation of silver nanoparticles (AgNPs).

To prepare AgNPs take the amount of the pomegranate peel extract, which was previously made in clause (2.3), and a few drops of sodium hydroxide 0.1 M were added to freshly prepared (PE) for PH adjusted to 8.0, at room temperature, silver nitrate solution with a (0.006) M concentration was added in droplets at temperature (25) °C. This color change to brown, indicative of the formation of silver nanoparticles, has a maximum absorbance (λ_{max}) at wavelengths between 420 and 460 nm (17).

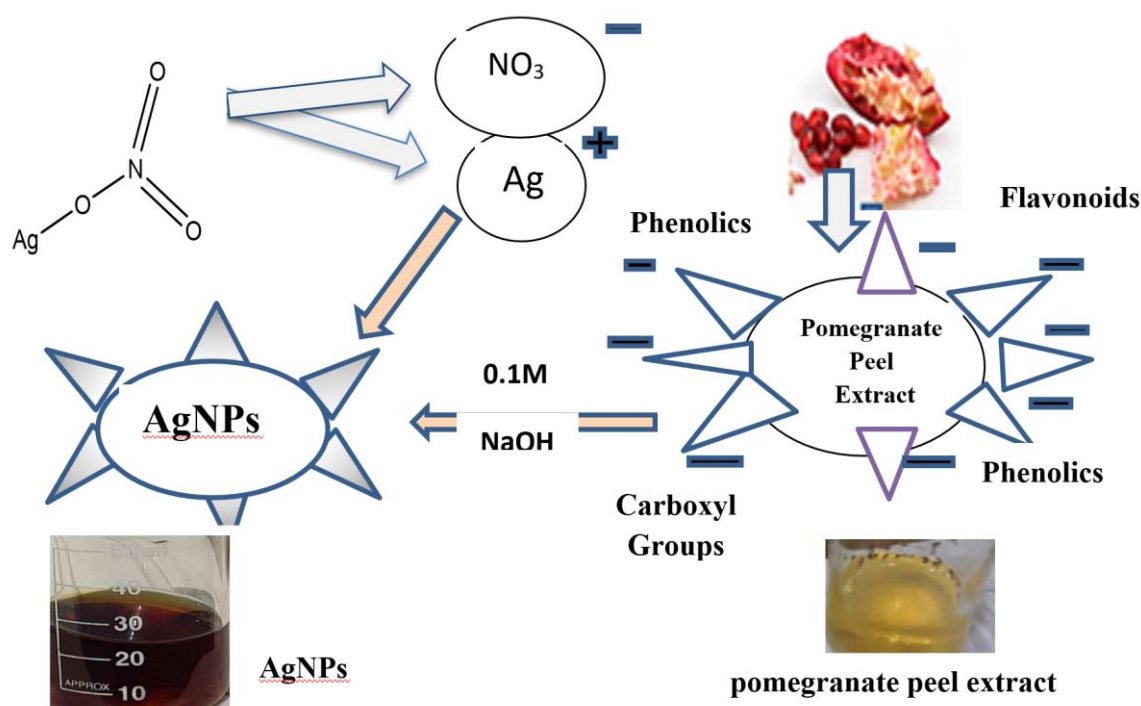


Figure 2: The suggested method for producing AgNPs using pomegranate peel extract.

2.5. Preparation of Ion-Pairs

The pair of ions was prepared by mixing 50 ml of the furosemide drug solution 0.1 M with 100 ml of silver nanoparticles (AgNPs), a light brown precipitate of (FUR-AgNPs) formed, and the precipitate was filtered using Whitman No. 1 filter paper. The precipitate was allowed to dry out at room temperature for two days.

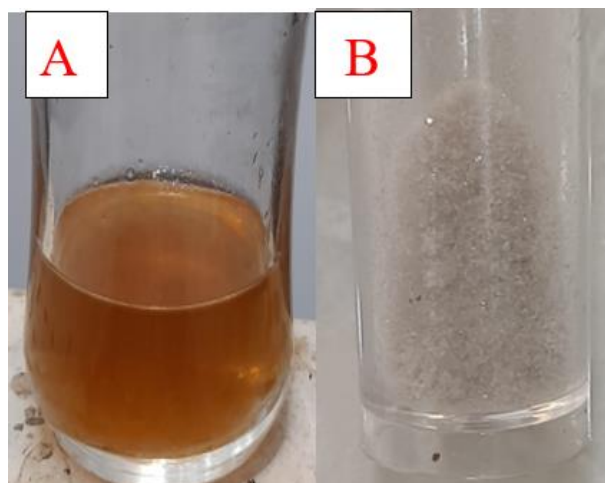


Figure 3: Ion pair (FUR-AgNPs) A: before and B: after filtrate.

2.6. Making a Coated Carbon Sensor

The sensor is prepared using a pure carbon rod using a thin polyethylene tube. The active membrane was applied to the sensors' surface by dipping one end in the coating solution. [0.1g ion-pair (FUR-AgNPs), 0.2 g polyvinyl chloride (PVC), 0.35 mL Plasticized dibutyl phthalate (DBP) and 5 mL THF] for several times, each time leaving the membrane to dry in the air for five minutes. The carbon rod's other end was left unconnected for connecting.



Figure 4: Coated Carbon Sensor.

3. Results and discussion

3.1. Characterization

3.1.1. UV-Visible Spectroscopy for silver nanoparticles

For the first characterization of produced nanoparticles, UV-vis spectroscopy is a very helpful and trustworthy method. It is also used to track the production and stability of AgNPs (18). Because of their distinctive optical characteristics, AgNPs significantly interact with certain light wavelengths (19). The generated silver nanoparticle solution was scanned at wavelengths between 300 and 800 nm, showing the maximum absorption at 452 nm, as shown in Figure 5, which is consistent with the creation of stable AgNPs that absorb between 420 and 460 nm.

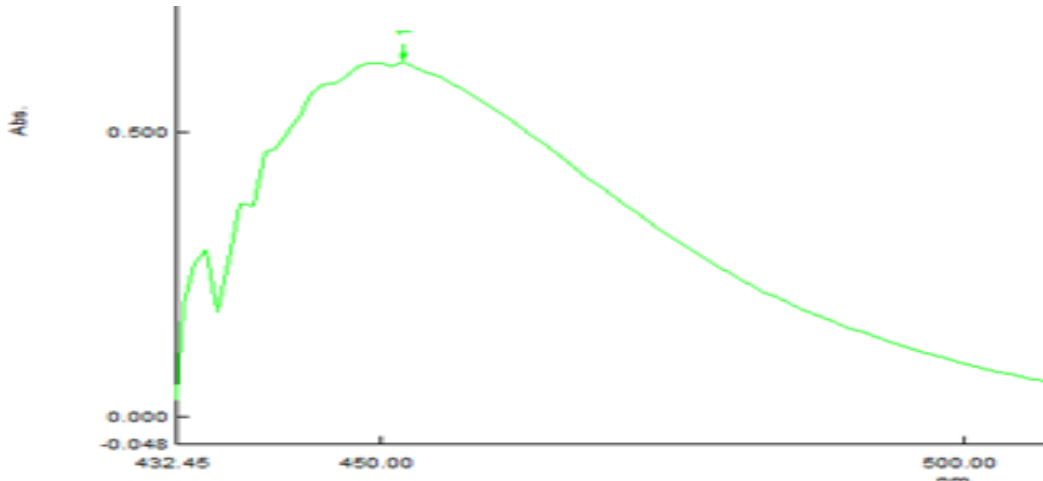


Figure 5: UV-VIS spectrum of silver nanoparticles.

3.1.2. Scanning Electron Microscopy (SEM)

SEM is A technique for surface imaging that can fully resolve various particle sizes, size distributions, forms of nanomaterials, and the surface. Data regarding surface morphology may be obtained using field emission scanning electron microscopy (FESEM). The particles for (AgNPs) had average diameters of 43.52 nm, 47.00nm, and 47.00 nm, varied particle sizes, size distributions, forms of nanomaterials, and the surface morphology of produced particles at the micro and nanoscales (20,21).

An SEM picture of silver nanoparticles using pomegranate peel extract is shown in Figure 6. With an assumption of 200 nanometers, the distribution of the particles is visible through the surface under examination and a spherical or semi-spherical shape.

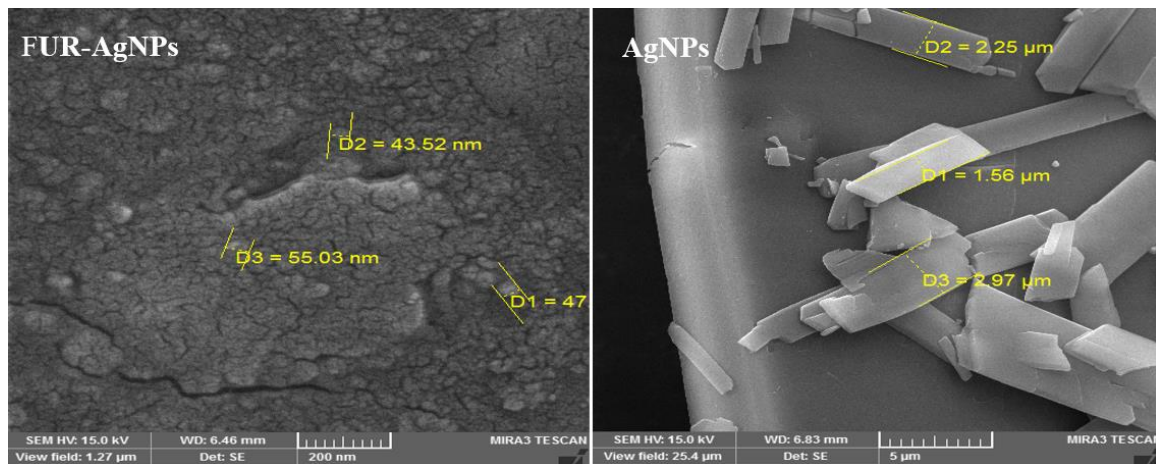


Figure 6: The X-ray diffraction patterns of silver nanoparticles (AgNPs).

3.1.3. Atomic Force Microscopy for silver nanoparticles (AgNPs).

AFM is often used to examine the size, shape, and structure of nanomaterials as well as their dispersion and aggregation. Three distinct scanning modes are available: contact mode, non-contact mode, and intermittent sample contact mode (22,23).

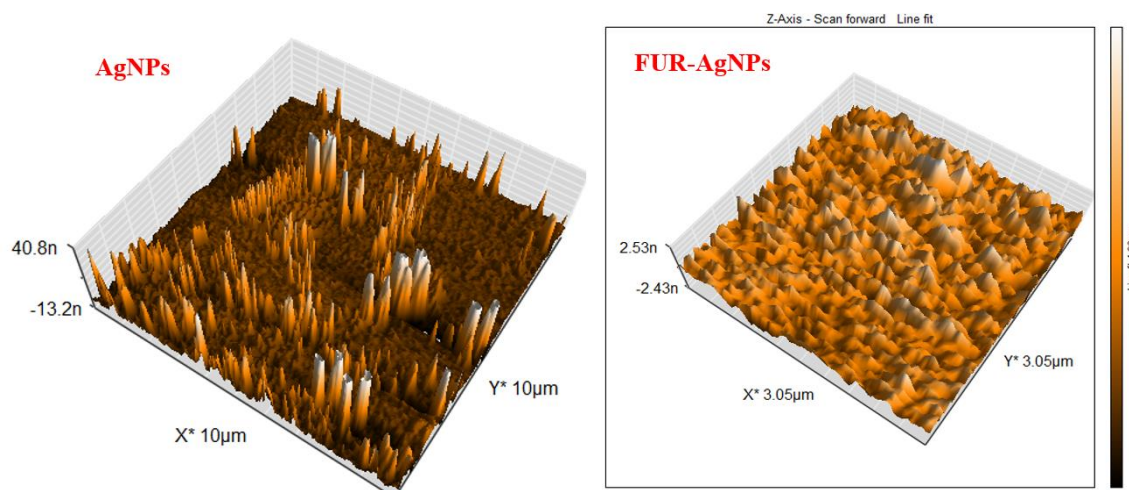


Figure 7: AFM of silver nanoparticles (AgNPs).

3.1.4. X-ray Diffraction (XRD).

A common analytical method that has been used to examine both molecular and crystal structures is X-ray diffraction (Figure 8; Table 1) (24). Qualitative identification of different chemicals and quantitative resolution of chemical species evaluating the degree of crystallinity (Figure 9; Table 2) (25), isomorphous substitutions, and particle sizes (26).

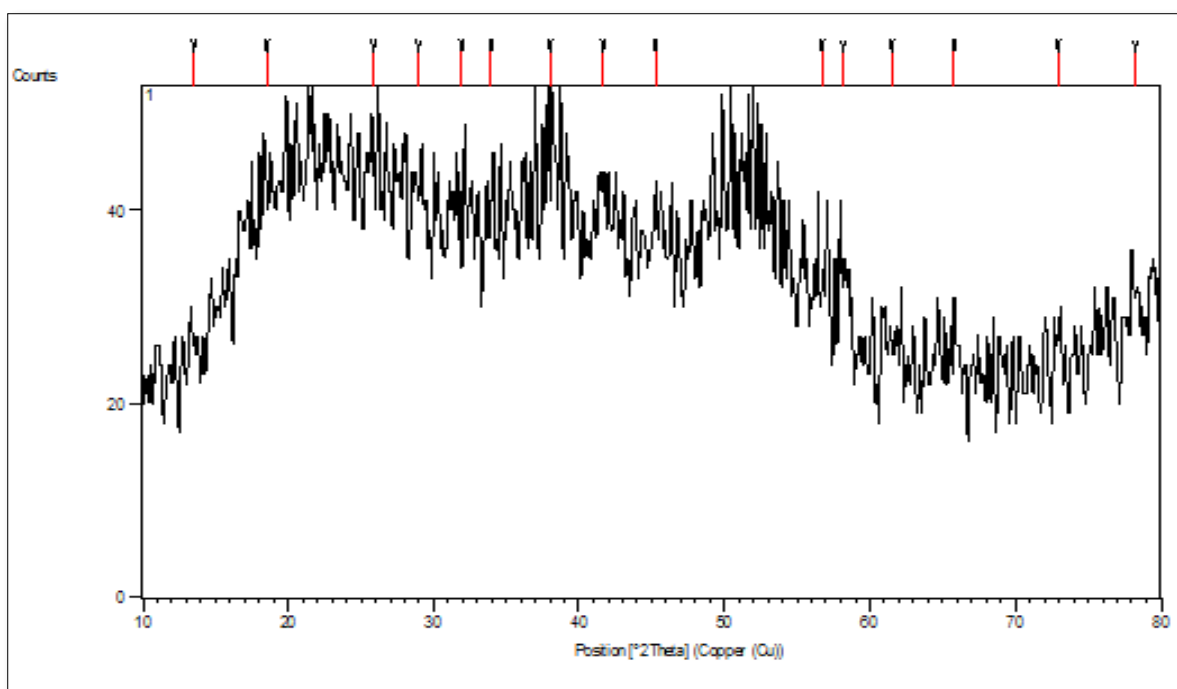


Figure 8: The X-ray diffraction patterns of silver nanoparticles (AgNPs).



Table 1: The X-ray diffraction results of silver nanoparticles (AgNPs).

Pos. [°2Th.]	Height [cts]	FWHM Left [°2Th.]	d-spacing [Å]	Rel. Int. [%]	Average D nm
13.48916	1.863711	0.7872	6.56433	21.56	10.62
18.51848	2.319751	0.5904	4.79135	26.83	14.41
25.86708	3.324218	0.5904	3.44444	38.45	14.43
28.96898	2.113935	0.5904	3.08229	24.45	14.52
31.94896	-2.80664	0.7872	2.80128	-32.47	10.97
33.94986	3.462925	0.5904	2.64062	40.06	14.7
37.9904	5.794628	0.5904	2.36855	67.03	14.87
41.63004	6.702356	0.7872	2.1695	77.53	11.28
45.24642	6.910831	0.492	2.00416	79.94	18.28
56.71115	4.082605	0.5904	1.62322	47.23	15.98
58.16952	6.973756	0.5904	1.58595	80.67	16.09
61.51439	2.895585	0.7872	1.5075	33.5	12.27
65.80708	8.644662	0.5904	1.41918	100	16.75
72.9515	4.732291	0.6888	1.29682	54.74	14.99
78.26392	3.152078	0.7872	1.22156	36.46	13.6
Average particle size (nm)					14.25067

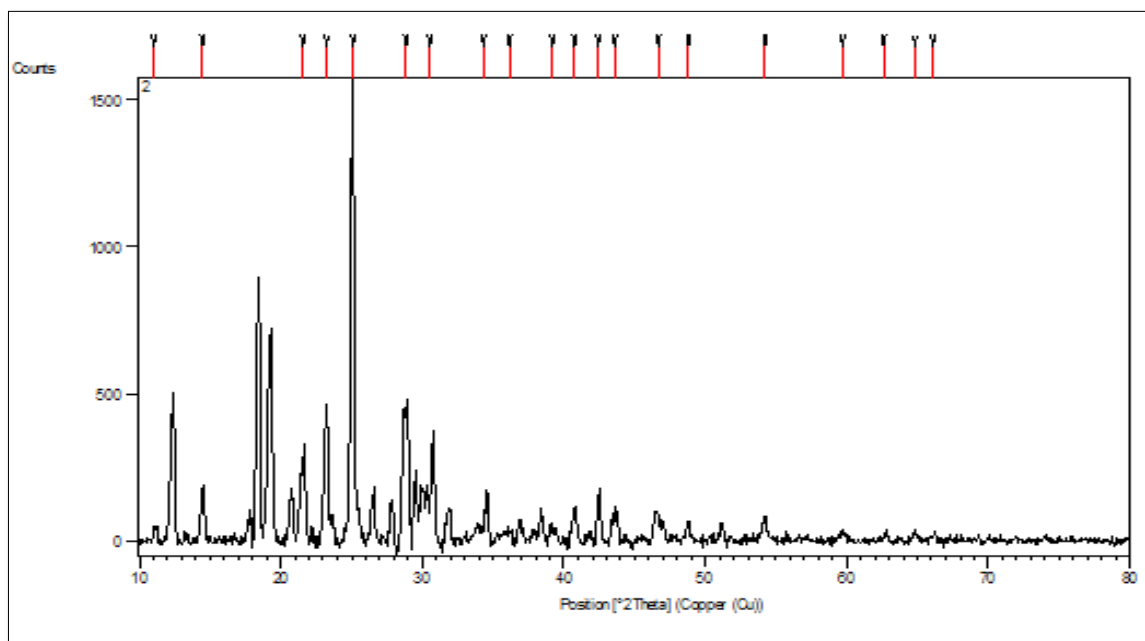


Figure 9: The X-ray diffraction patterns of Nanoprecipitate (FUR-AgNPs).

Table 2: The X-ray diffraction results of Nanoprecipitate (FUR-AgNPs).

Pos. [°2Th.]	Height [cts]	FWHM Left [°2Th.]	d-spacing [Å ^o]	Rel. Int. [%]	D (nm)
11.02187	12.23349	0.5904	8.02761	1.01	14.12
14.46631	154.1723	0.5904	6.12305	12.72	14.17
21.57012	269.3148	0.5904	4.1199	22.22	14.31
23.24448	294.6426	0.5904	3.82679	24.31	14.35
25.08214	1211.845	0.5904	3.55043	100	14.4
28.85198	430.8432	0.492	3.09453	35.55	17.42
30.50201	156.5932	0.5904	2.93078	12.92	14.57



34.30908	46.97189	0.984	2.61379	3.88	8.83
36.16368	29.30539	0.5904	2.48389	2.42	14.79
39.1941	21.76444	0.492	2.29854	1.8	17.91
40.74803	101.7266	0.492	2.2144	8.39	18
42.41311	94.08075	0.5904	2.13124	7.76	15.08
43.57839	86.81773	0.492	2.07692	7.16	18.17
46.67453	71.17764	0.5904	1.94611	5.87	15.31
48.81657	36.03094	0.5904	1.86561	2.97	15.44
54.21526	57.89527	0.5904	1.6919	4.78	15.8
59.70591	26.56285	0.492	1.54876	2.19	19.45
62.60322	10.24025	0.5904	1.48388	0.85	16.46
64.82026	26.03016	0.492	1.43838	2.15	19.99
66.09300	14.37802	0.492	1.41373	1.19	20.13
Average particle size (nm)					15.935

3.1.5. Fourier Transform Infrared (FTIR) Spectroscopy.

In academic and commercial research, FTIR spectroscopy is commonly employed to determine if biomolecules contribute to the creation of nanoparticles (27-28). The organic groups responsible for the creation of silver nanoparticles were discovered using pomegranate peel extract and infrared light. The FT-IR spectrum revealed the presence of an O-H group at a frequency of 3436 cm^{-1} , indicating the presence of alcohol in the pomegranate peel extract, while (polyols, hydroxyflavones), and (c-c) at a frequency of 1637.90 cm^{-1} indicate the presence of an aromatic component in the pomegranate peel extract.

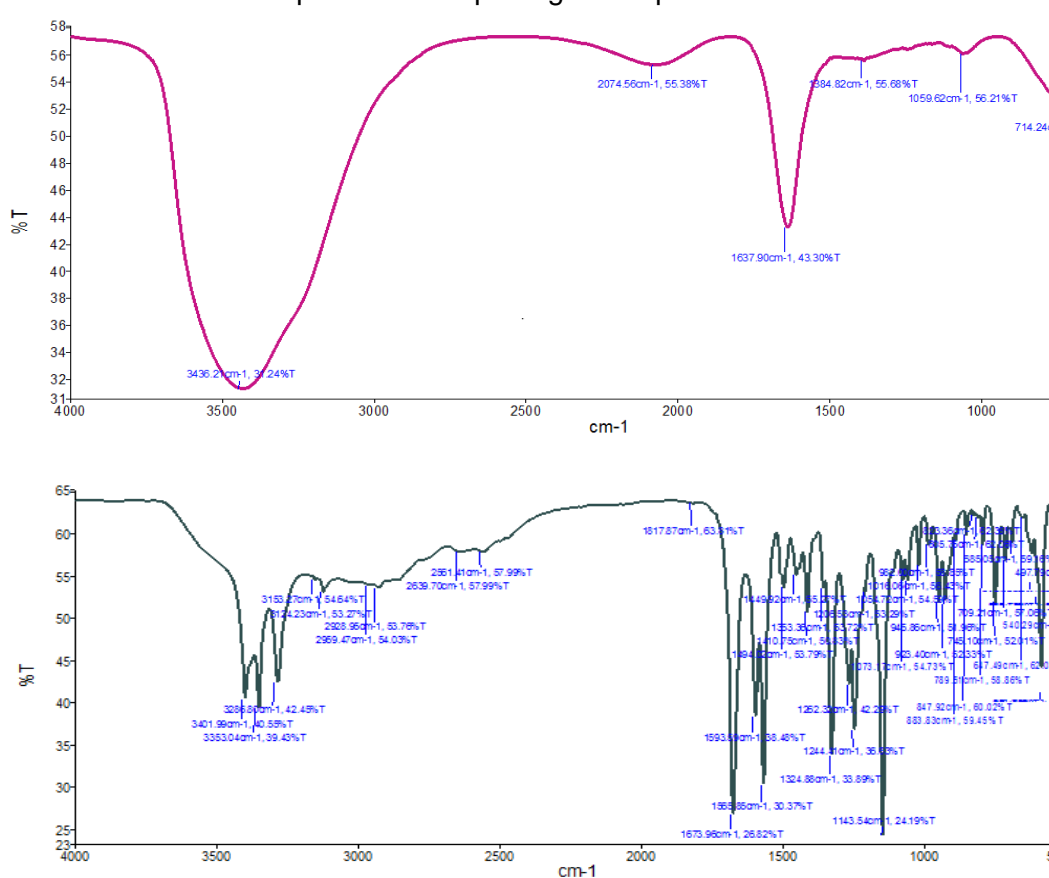


Figure 10: FTIR spectrum of silver nanoparticles above and Nanoprecipitate down (FUR-AgNPS).



3.2. Study of optimal conditions for Nano electrodes.

3.2.1. Effect of pH.

To determine the ideal pH function value at which the manufactured nanoelectrode operates using concentrations 1×10^{-3} and 1×10^{-6} M of FUR drug at various pH values 1-9. Small amounts of HCl or NaOH solution were added to the solution to change the pH. 0.1-1 M of each. Every pH level's potential was noted. The ideal pH range is between 3-6 electrodes with a pH-independent potential. However, at pH levels greater than 5 the potential decreases gradually for AgNPs-FUR. It's important to remember that a white precipitate forms at pH levels higher than 7, and that causes a potential decrease. At pH levels less than 2, the potential values decrease, which can be due to the interference of hydronium ions.

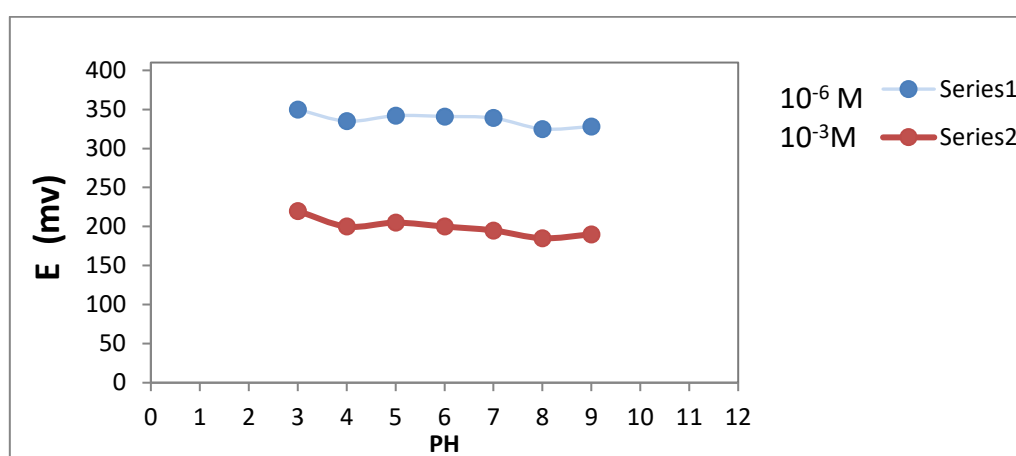


Figure. 11: The Effect of acid function on the drug (FUR).

3.2.2. Effect of Temperature.

The potential change was determined by varying the temperature of the drug solution from 10-50 °C for concentrations of 1×10^{-3} and 1×10^{-6} M FUR. The relationship of the measured potential with temperature. The results in Fig. 12 demonstrated that the electrode's optimal operating temperature is 10-50 °C.

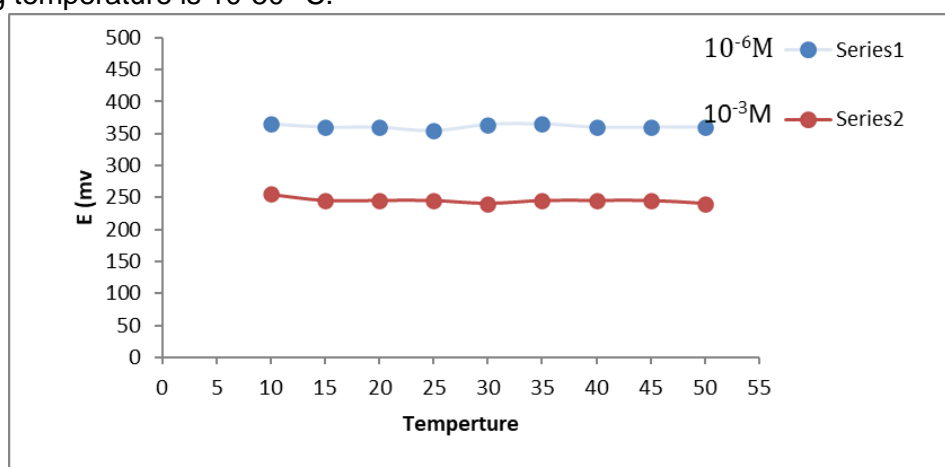


Figure 12: Effect of temperature on the response of electrodes.



3.2.3. Calibration Plot of the Fabricated Electrodes and Limit of Detection.

The developed electrode (AgNPs-FUR) and a Calomel reference electrode were immersed in FUR solutions within the concentration range of 1.0×10^{-8} - 1.0×10^{-1} M. The plot of E (mV) against $-\log [\text{FUR}]$ is depicted in Figure 13. A linear response is shown by the electrode across the concentration ranges from 1.0×10^{-6} - 1.0×10^{-1} M having -61.286 mV/decade for AgNPs-FUR almost Nernstian slopes, and LOD values for the AgNPs-FUR electrode is 3.62×10^{-8} M demonstrating that the sensors being studied are very sensitive and useful for detecting traces of FUR drug.

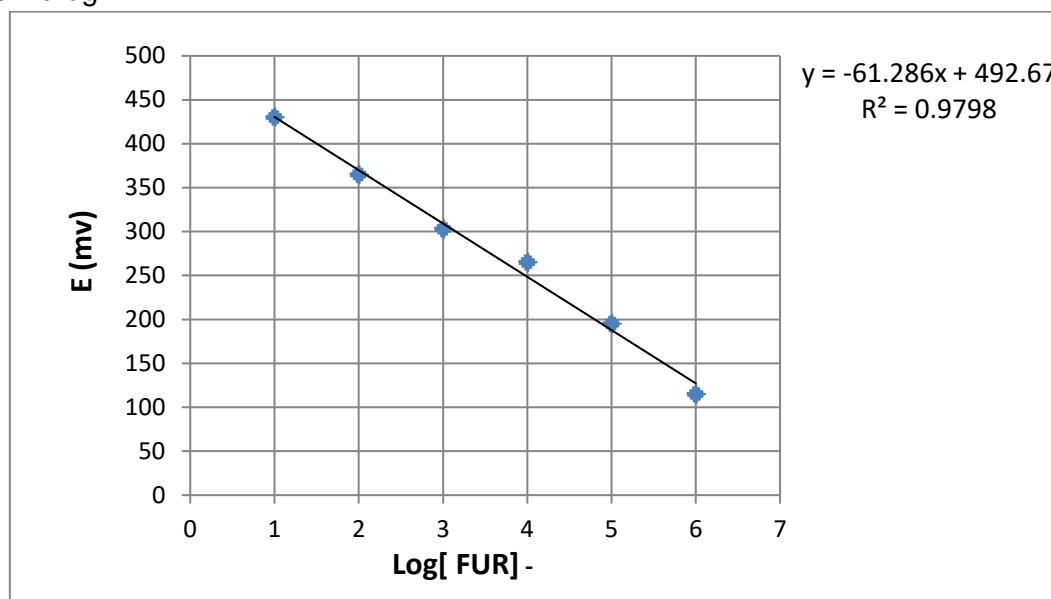


Figure 13: Standard curve of AgNPs-FUR electrode.

3.2.4. Life Time and Response Time.

In order to determine the (AgNPs-FUR) electrode's storage stability and obtain the best results, the potentiometric measurements were performed numerous times each week at the ideal pH and temperature. According to the results, AgNPs-FUR electrodes can be utilized for 75 days without experiencing a discernible change in potential. The IUPAC defines response time as the amount of time needed from the instant the (AgNPs-FUR) electrode and the drug solution's calomel electrode come into contact with the steady state with a potential change of ± 1 mv. The newly coated carbon's response time was 35 seconds at concentrations of 1.0×10^{-6} M for the AgNPs-FUR electrode and 5 seconds for 1.0×10^{-1} M of concentration, and the AgNPs-FUR electrode new coated carbon had the quickest reaction time, measuring 5 seconds for 1.0×10^{-1} M and 35 seconds for 1.0×10^{-6} M. as shown in Fig. 14.

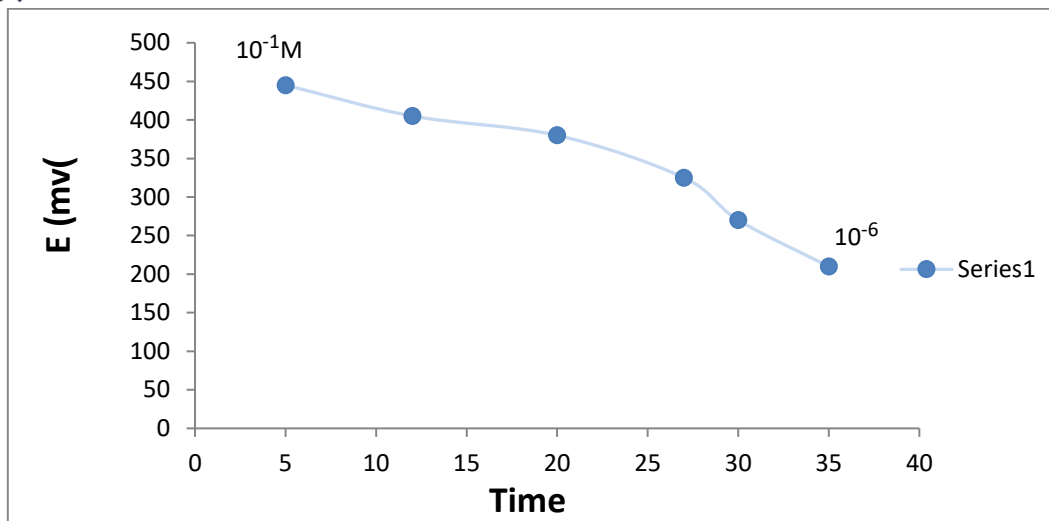


Figure 14: Response time of AgNPs-FUR electrode.

3.2.5. Precision and Accuracy.

Analyses were performed on two distinct levels (within the practical limitations) of pure and pharmaceutical drug solutions to assess the precision and accuracy of the suggested approach. Every solution was applied five times. The determined percent relative standard deviation (RSD%) served as the basis for precision and accuracy and the value of the RSD% cannot be more than 1.208. Table 3 findings demonstrate the excellent precision and accuracy of this technique.

3.2.5. Analytical Applications.

A direct calibration approach was employed to assess the levels of furosemide in both pure and pharmaceutical forms. After the electrodes were manufactured, the findings were expressed as the recoveries %. To determine FUR pure drug solutions, the percentage average recoveries are 100.267 % for the AgNPs-FUR electrode. The determination of FUR tablets (LASIX 40 mg tablet) % recoveries is 100% for electrodes, as shown in Table 3.

Table 3: Data processing using statistics to determine FUR in pharmaceutical and pure forms using new AgNPs-FUR electrode.

Sample	FUR			
	Taken (mol/L)	Found (mol/L)	RSD%	Rec%
Pure drug	1×10^{-1}	0.957×10^{-1}	0.88	95.70
	3×10^{-3}	1.038×10^{-3}	1.09	103.80
	6×10^{-6}	1.013×10^{-6}	1.208	101.30
n	5			
% RE	-0.45			
Lasix 40 mg	1×10^{-2}	1.03×10^{-2}	0.50	103
	1×10^{-4}	1×10^{-4}	0.28	100
	1×10^{-6}	9.7×10^{-7}	0.30	97
n	5			
% RE	0.79			



4. Conclusions

An ion-selective electrode was added in the suggested approach for the determination of FUR. Constructed using a PVC matrix, DBP as a plasticizer, and AgNPs as the active ingredients. This electrode demonstrated a successful application with a strong recovery rate and a low detection limit. Additionally, the electrode lifetime, quick response, strong selectivity, and manageable operating concentration range.

References

1. Abdel-Hamid, M. E. (2000). High-performance liquid chromatography–mass spectrometric analysis of furosemide in plasma and its use in pharmacokinetic studies. *Il Farmaco*, 55(6-7), 448-454.
2. van Mil, J. W. F. (2014). Alison Brayfield (Editor-in-Chief): Martindale, the complete drug reference.: The pharmaceutical Press, London, 2014, ISBN: 978 0 85711 139 5.
3. Pharmacopoeia, B. (2013). British pharmacopoeia commission London; the department of health. Social Services and Public Safety, 1, 719-720.
4. Marles, R. J., Barrett, M. L., Barnes, J., Chavez, M. L., Gardiner, P., Ko, R., ... & Griffiths, J. (2011). United States pharmacopeia safety evaluation of Spirulina. *Critical reviews in food science and nutrition*, 51(7), 593-604.
5. Haas, M., & Forbush III, B. (2000). The Na-K-Cl cotransporter of secretory epithelia. *Annual review of physiology*, 62(1), 515-534.
6. Shankar, S. S., & Brater, D. C. (2003). Loop diuretics: from the Na-K-2Cl transporter to clinical use. *American Journal of Physiology-Renal Physiology*, 284(1), F11-F21.
7. Odland, B. (1979). Relationship between tubular secretion of furosemide and its saluretic Effect. *The Journal of pharmacology and experimental therapeutics*, 208(3), 515-521.
8. de Lima Benzi, J. R., Rocha, A., Colombari, J. C., Pego, A. M. G., dos Santos Melli, P. P., Duarte, G., & Lanchote, V. L. (2023). Determination of furosemide and its glucuronide metabolite in plasma, plasma ultrafiltrate and urine by HPLC-MS/MS with application to secretion and metabolite formation clearances in non-pregnant and pregnant women. *Journal of Pharmaceutical and Biomedical Analysis*, 235, 115635.
9. Karunakaran, A., Sudharsan, S. I., Jayaprakash, R., Vekatachalam, S., Raju, S. K., & Elampulakkadu, A. (2021). Analytical method development and validation for the estimation of furosemide an anti-diuretic in Furosemide injection diluted with normal saline in presence of impurities by RP-HPLC. *Brazilian Journal of Biological Sciences*, 8(18), 35-56.
10. Aljanabi, W. H. H., Salman, S. A., & Ahmed, S. A. (2018). A comparative study for estimation of Losartan Potassium drug by atomic absorption technique and UV-visible spectrophotometry. *Tikrit Journal of Pure Science*, 23(9), 67-70.
11. Martins, T. S., Bott-Neto, J. L., Raymundo-Pereira, P. A., Ticianelli, E. A., & Machado, S. A. (2018). An electrochemical furosemide sensor based on pencil graphite surface modified with polymer film Ni-salen and Ni (OH) 2/C nanoparticles. *Sensors and Actuators B: Chemical*, 276, 378-387.
12. Shetti, N. P., Sampangi, L. V., Hegde, R. N., & Nandibewoor, S. T. (2009). Electrochemical oxidation of loop diuretic furosemide at gold electrode and its analytical applications. *International Journal of Electrochemical Science*, 4(1), 104-121.



13. Gadepalli, S. G., Deme, P., Kuncha, M., & Sistla, R. (2014). Simultaneous determination of amlodipine, valsartan and hydrochlorothiazide by LC–ESI-MS/MS and its application to pharmacokinetics in rats. *Journal of pharmaceutical analysis*, 4(6), 399-406.
14. Schluesener, J. K., & Schluesener, H. J. (2013). Nanosilver: application and novel aspects of toxicology. *Archives of toxicology*, 87, 569-576.
15. Jaswal, T., & Gupta, J. (2023). A review on the toxicity of silver nanoparticles on human health. *Materials Today: Proceedings*, 81, 859-863.
16. Pratsinis, A., Hervella, P., Leroux, J. C., Pratsinis, S. E., & Sotiriou, G. A. (2013). Toxicity of silver nanoparticles in macrophages. *Small*, 9(15), 2576-2584.
17. Fu, L. M., Hsu, J. H., Shih, M. K., Hsieh, C. W., Ju, W. J., Chen, Y. W., ... & Hou, C. Y. (2021). Process optimization of silver nanoparticle synthesis and its application in mercury detection. *Micromachines*, 12(9), 1123.
18. Sastry, M., Patil, V., & Sainkar, S. R. (1998). Electrostatically controlled diffusion of carboxylic acid derivatized silver colloidal particles in thermally evaporated fatty amine films. *the journal of physical chemistry B*, 102(8), 1404-1410.
19. Kennedy, A. J., Wu, Q., Kremer, K., & Gibbons, S. (2019). Determination of fluorescence emission and UV-Vis-NIR absorbance for nanomaterials solution using a HORIBA Scientific NanoLog® spectrofluorometer.
20. Yao, H., & Kimura, K. (2007). Field emission scanning electron microscopy for structural characterization of 3D gold nanoparticle superlattices. *Modern research and educational topics in microscopy*, 2, 568-576.
21. Pawley, J. B. (1997). The development of field-emission scanning electron microscopy for imaging biological surfaces. *SCANNING-NEW YORK AND BADEN BADEN THEN MAHWAH-*, 19, 324-336.
22. Song, J., Kim, H., Jang, Y., & Jang, J. (2013). Enhanced antibacterial activity of silver/polyrhodanine-composite-decorated silica nanoparticles. *ACS applied materials & interfaces*, 5(22), 11563-11568.
23. Picas, L., Milhiet, P. E., & Hernández-Borrell, J. (2012). Atomic force microscopy: A versatile tool to probe the physical and chemical properties of supported membranes at the nanoscale. *Chemistry and physics of lipids*, 165(8), 845-860.
24. Das, R., Nath, S. S., Chakdar, D., Gope, G., & Bhattacharjee, R. J. J. O. N. (2009). Preparation of silver nanoparticles and their characterization. *Journal of nanotechnology*, 5, 1-6.
25. Cabral, M., Pedrosa, F., Margarido, F., & Nogueira, C. A. (2013). End-of-life Zn–MnO₂ batteries: electrode materials characterization. *Environmental technology*, 34(10), 1283-1295.
26. Singh, D. K., Pandey, D. K., Yadav, R. R., & Singh, D. (2013). A study of ZnO nanoparticles and ZnO-EG nanofluid. *Journal of Experimental Nanoscience*, 8(5), 731-741.
27. Gurunathan, S., Han, J. W., Kwon, D. N., & Kim, J. H. (2014). Enhanced antibacterial and anti-biofilm activities of silver nanoparticles against Gram-negative and Gram-positive bacteria. *Nanoscale research letters*, 9, 1-17.
28. Perevedentseva, E. V., Su, F. Y., Su, T. H., Lin, Y. C., Cheng, C. L., Karmenyan, A. V., & Lugovtsov, A. E. (2010). Laser-optical investigation of the Effect of diamond nanoparticles on the structure and functional properties of proteins. *Quantum Electronics*, 40(12), 1089.